

## Combined heat and power generation of the hydrogen chain based on MYRTE platform

Auline Rodler, Pierrick Haurant, Ghjuvan-Antone Faggianelli, Guillaume Pigelet, Philippe Poggi

University of Corsica, UMR SPE CNRS 6134, F-20000 Ajaccio, France

### Abstract

The objective of this paper is to present the thermal recovery system of the MYRTE hydrogen chain. This system recaptures the thermal energy produced by the proton exchange membrane (PEM) fuel cell (100 kW) and a PEM electrolyzer (10 Nm<sup>3</sup>/h). The recovery system must insure to maintain the set point temperature of the inlet cooling water to the facilities. In that view, the heat is collected and stored in a water storage tank and the rest is dissipated using a turbofan. In this paper, the power dissipated and stored in the recovery system is evaluated based on measurements. The results show that the fuel cell generates at its maximal electrical power an equivalent amount of thermal power. Finally, a model coupling the fuel cell and the heat recovery system is implemented in TRNSYS®, showing a good agreement to the measurements.

Keywords: Co-generation, Hydrogen, Fuel cell, Electrolyzer, Solar energy

---

### 1. Introduction: Energy Context in Corsica

Corsica Island is located in the Genova gulf in the Mediterranean Sea and therefore exposed to the Mediterranean climate, characterized by hot and dry summers and mild and humid winters. Its solar energy potential is one of the most important of France. As Corsica is very hilly in the centre, we can find different climates via the island. The solar resource distribution is very heterogeneous and the solar radiation can be very fluctuating.

Besides, the Corsican electrical grid is typical of an insular electrical network: it is weakly connected to the mainland grid, small-sized and sensitive to variations in electrical production. The threshold of maximum 30% of integration of fatal intermittent production, fixed by the French law to insure the insular grid's stability, was overpassed in 2012<sup>1</sup>. However, photovoltaic plants projects are still considered.

Therefore, storage systems to smooth the intermittency of the solar production seem necessary. Hydrogen production and consumption can help to manage electrical power fluctuations of intermittent renewable energy sources integrated into the electrical grid.

In this context, the hybrid MYRTE (mission hydrogen for the integration of renewable into the electrical grid) demonstration platform has been built: it combines a photovoltaic array and a hydrogen chain used as a storage solution.

### 2. The hydrogen solution: MYRTE project

The first aim is to test hydrogen storage solutions as an alternative to the peak shaving of electrical demand (Darras, 2010). Another aim of this platform is to monitor the photovoltaic power output smoothing and to reduce the PV fluctuations (Darras et al., 2012). Finally, the development of algorithms and optimal strategy

---

<sup>1</sup> <http://corse.edf.com/edf-en-corse/nos-energies/nos-energies-48454.html>

management coupling the processes (PV production – Hydrogen chain) is another target.

### 2.1 Presentation of the experimental platform

The experimental MYRTE platform is a technological platform dedicated to the coupled studies between PV/hydrogen chains. This platform has been inaugurated on January 2012.

MYRTE platform is composed of the following sub systems (Fig. 1):

- A photovoltaic array of 560 kW<sub>p</sub> (3700 m<sup>2</sup> covered by 2240 PV TENESOL TE2200 modules);
- 28 DC/AC three-phase 17 kW inverters (SMA SUNNY TRIPOWER 17000TL);
- The fuel cell subsystem (SSPAC), composed of a PEM (proton exchange membrane) fuel cell with a power of 100 kW supplied by AREVA ;
- The subsystem electrolyser (SSEL), composed of a PEM electrolyzer of a nominal power of 50 kW with a H<sub>2</sub> flowrate which can reach 10 Nm<sup>3</sup>/h, developed by AREVA ;
- The storage subsystem, composed of drying and purification systems of gases as well as two H<sub>2</sub> storage tanks and one O<sub>2</sub> tank (GLI ETS Citergaz) each with a volume of 28 m<sup>3</sup>, under a maximal pressure of 35 bars (1400 Nm<sup>3</sup> d'H<sub>2</sub> and 700 Nm<sup>3</sup> d'O<sub>2</sub>) ;
- A 800 kVA transformer to inject electrical production on the high voltage network ;
- The thermal recovery subsystem to recover heat from the electrolyzer and the fuel cell to maintain the operative temperature of both systems.

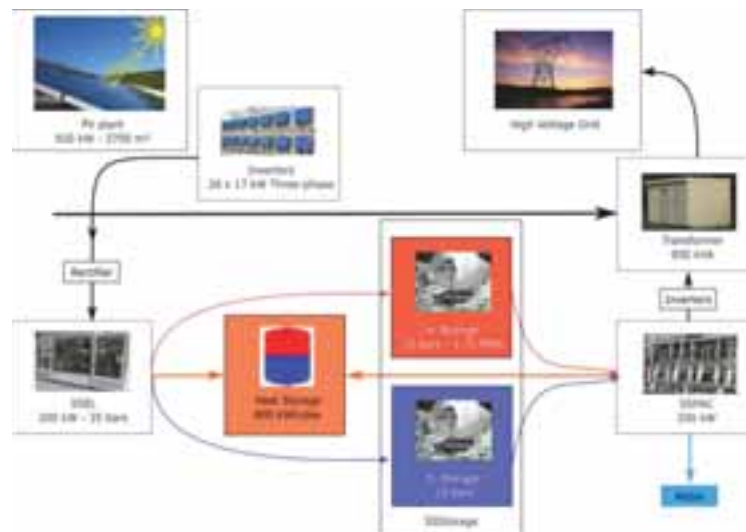


Figure 1: Operating of MYRTE

The electrical mean efficiency of the hydrogen chain is of about 23 – 25 %. The facilities as the fuel cells release heat when they generate electricity and are therefore interesting for combined heat and power (CHP) applications, also known as cogeneration. CHP hydrogen system time-averaged electrical, thermal and global (combining both heat and electrical powers) efficiencies have been evaluated by Hwang et al. (2013) to about 37 %, 24 % and 61 % respectively. To conclude, recovering the thermal heat of fuel cell systems strongly increases the overall energy efficiency of the global system.

### 2.2 Heat recovery

To increase the global efficiency of the hydrogen chain, the heat recovery system is composed of a thermal energy storage system to store the heat produced by the fuel cell (FC) and electrolyzer (EL). This heat can then be used in a secondary loop, for example for a residential application.

The cooling loop will systematically act on both electrolyzer and fuel cell, that is, the water passes through their heat exchangers to guaranty the operating temperature which is 60 °C for the electrolyzer and 70 °C for the fuel cell. The maximal overall operating temperature not to overpass is fixed to 75 °C, for security reasons. The absorbed heat is then stored or dissipated by turbofans (Fig 2). The glycolic liquid is kept in movement

by a pump (KQ500) and goes to the heat exchanger of the tank where the heat can be stored. The maximal temperature of the water which will go back to the electrolyzer and fuel cell is fixed in between 35 – 40 °C. This set point temperature is ensured by turbofans which will dissipate the heat if the sensor KT501 indicates a temperature above the set point temperature. The cooling overall flow rate depends on the electrolyzer or fuel cell system working order and depends on the opening percentage of the regulation valves. For the moment, the experimental set up is not connected to any secondary loop which could allow exploiting the heat. As seen on the schematic drawing of the thermal recovery system (Fig.2), the water can follow different paths in the circuit. It is possible to cool down the electrolyzer and fuel cell systems, to recover the heat from them and exploit it or absorb the heat without recovering it.

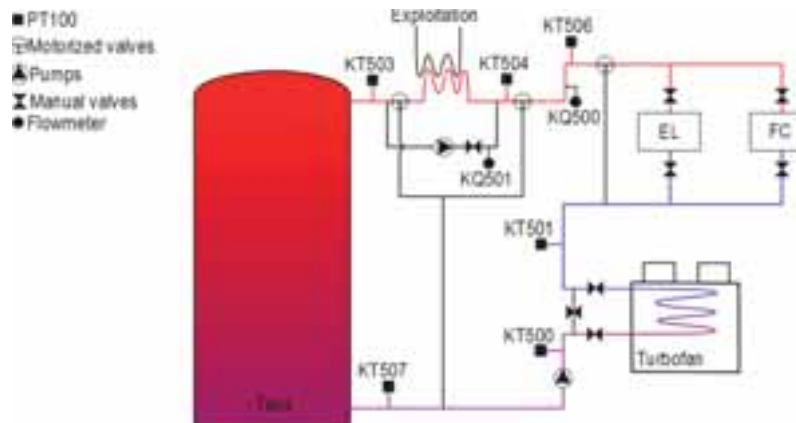


Fig. 2: Heat recovery system of the hydrogen chain platform

Different modes in the circuit are possible:

- **Mode to cool down the system** which is ordered by the control system. Different cases are possible depending if the storage is full and depending on the water temperature of the sensor KT501 placed before electrolyzer and fuel cell heat exchangers:
  1. If the storage is not full and  $KT501 < \text{set point temperature (35 } ^\circ\text{C)}$ : we will store the heat;
  2. If the storage is not full and  $KT501 > \text{set point temperature}$ : we will store the heat and dissipate the heat by the two turbofans;
  3. If the storage is full and  $KT501 > \text{set point temperature}$ : the turbofan is used (frequency of the fan is function of the overtaking of the set point temperature);
  4. If the storage is full and  $KT501 < \text{set point temperature}$ : the turbofan is used (at its minimal working).
- **Mode to recover the heat to a second water circuit:** the system would allow the water to go to a second circuit. The water would be in between 45 and 55°C for the heating system of a building. Until now, this mode is not possible as there is no connection to a building.
- **Mode to take out the heat without recovering the heat:** the heat is transferred to the storage tank and to the turbofan.
- **Stopping mode or manual mode.**

### 3. Modelling

#### 3.1 Presentation of the measurements feedback

In this paper, we present results for a three day period in May 2014, when the platform was working in a peak shaving mode: each day, the electrolyzer consumed 46 kW during the day and the fuel cell produced a maximum of 95 kW between 08.30 pm and 10.30 pm (Fig. 3). The peak shaving mode consists in using additional sources of energy at moments when the electricity demand is important. That is, the MYRTE platform is used at moments of peak shaving: the fuel cell is used to supply electricity to the grid. The heat recovery system is turned on only when the electrolyzer or fuel cell is operating. The set point temperature of the KT501 was fixed to 35°C.

The heat recovery system is turned on only when the electrolyzer or fuel cell are used. The set point temperature of the KT501 was fixed to 35°C. For the moment, the experimental set up is not connected to any secondary loop which could allow exploiting the heat.

The electrical power generated by the fuel cell and the power consumed by the electrolyzer were measured (Fig. 3) as well as different temperatures (KT506, KT507 and KT501 show in Fig. 3). The outside temperature was also measured and a flowmeter gave the flowrate in the recovery loop. All measures are given at a minute time step.

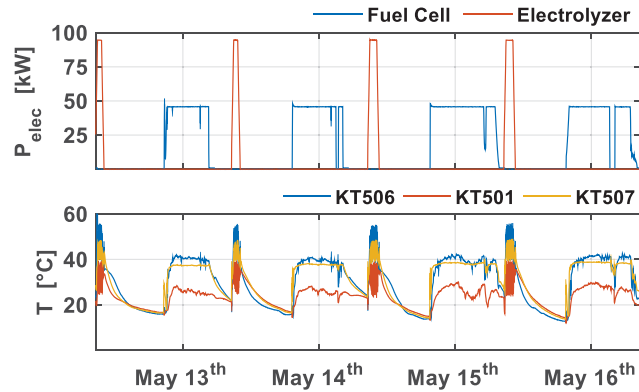


Figure 3: Electrolyzer and fuel cell electrical power

We can observe in Fig. 3 that the inlet fluid temperature in the thermal recovery system, measured by sensor KT506:

- reaches 40°C to 42°C when the electrolyzer works;
- varies between 41°C and 53°C when the fuel cell works.

Whatever the time considered, these temperatures are below the optimal temperatures of both systems, and far from their maximal operating temperatures: the hydrogen systems seem to be cooled down too much.

Besides, these fluid temperature ranges indicate that the heat recovered could be used for residential applications, as for the heating or pre-heating systems.

The fluid temperature decreases from 2 to 3 °C when the electrolyzer works and from 5 to 7 °C when the fuel cell works when it passes through the storage tank. Then, the water circulates through the turbofan and its temperature decreases strongly whatever its input temperature. When the electrolyzer works, the glycolic water temperature drops always below 30°C when measured on KT501. It oscillates between 32°C and 38°C when the fuel cell is on. The turbofan dissipates too much heat since it is oversized or not well controlled, so that the heat recovery system overcools the systems.

### 3.2 Sub-system parametrisation

A transient model adapted to the case study MYRTE, and particularly to the heat recovery system, is being developed using TrnSys® (TRNSYS, 1996). It is a software with a modular structure dedicated to dynamical simulation of complex energy systems. It aims at considering the global system composed by a set of interconnected subsystems modelled in 'types'. The thermal behaviour of the sub-systems has been modelled thanks to 'types' stemming from TRNSYS library (Tab. 1).

Table 1 Elements of TRNSYS model

Elements	Type	Comment
Data reader	9	Flowrate, ambient temperature, fuel cell control signal and electrolyzer control signal
Pipe	31	Hypothesis on the sizes and the thermal losses
Turbofan	Macro	Pipe and forced convection simulated
Water Tank	60d	With internal exchangers and taken into account the stratification (20 nodes)
Electrolyzer	Macro	Only the thermal aspect of the electrolyzer is considered
Fuel cell	170 k	FC O <sub>2</sub> /H <sub>2</sub> controlled with the intensity

The inputs of the model are:

1. the outdoor temperature ;
2. the flowrate of the glycolic fluid (KQ500);
3. heat generated by the electrolyzer.

The outputs of the model are:

1. the water temperature before, in and after the storage tank ;
2. the inlet and outlet temperature of the turbofan ;
3. the power and energy dissipated by the turbofan ;
4. the power and energy stored by the tank.

### 3.2.1 Tank

The water storage tank was modelled by using the Type 60d, which is a dynamical model for thermal stratified storage. It includes heat exchangers and auxiliary heaters. In this model, the tank is divided in N volumes or nodes. The water temperature for node i is evaluated according to the energy balance (Eq.1):

$$m_{w,i}c_p \frac{dT_{w,i}}{dt} = Q_{HEX,i} + Q_{AUX,i} + Q_{loss,i} + Q_{cond,tank,i} + Q_{conv,tank,i} + Q_{fconv,inout,i} \quad (\text{eq. 1})$$

where

- $Q_{HEX,i}$  and  $Q_{AUX,i}$  are the heat from the exchanger and auxiliaries
- $Q_{loss,i}$  is the thermal losses to the outside
- $Q_{cond,tank,i}$  is the thermal exchanges by conduction of the fluid in the tank between node i and nodes i + 1 and i - 1
- $Q_{conv,tank}$  is the thermal exchanges due to convection in the tank
- $Q_{conv,inout}$  is the bleedoff exchanges and the exchanges of the water supply in the tank to the N inputs/outputs of the tank.

This model is dynamic and zonal as it calculates the thermal transfers between control volumes, so it considers the stratification in the tank. The parametrization of the tank is sensitive as the geometry of its heat exchanger is particular. The tank is composed of 4 connected metal plates filled in with water and in contact with the exterior surface of the tank. The water tank is 4m high and has a 2m diameter, with a total volume reaching 14 m<sup>3</sup>.

The circulation of the fluid for this type of exchanger and the heat exchanges by conduction with the water of the tank differ from the exchanges of a tank with a coil. The circulation speed is smaller whereas the contact surfaces are more important. This is why we have considered a very long exchanger and we have overestimated the thermal exchange coefficients.

### 3.2.2 Electrolyzer

In TrnSys we do not have a 'type' modelling the electrolyzer PEM so that in this study the electrolyzer has

been considered as a constant heating source when operating. The heat has been evaluated from differences between the measured KT501 and KT506 temperatures.

This first very simple modelling does not allow simulating the thermal dynamic behaviour of the heat recovery system of MYRTE in a reliable way. The model validation will have a critical sense only when the fuel cell is operating. It is necessary that the model evaluates several levels of temperatures and heat supply. However, this simple modelling is necessary so that the global model can evaluate the average heat generated by the electrolyzer and can insure a continuity through the simulations between each operating period of the fuel cell.

### 3.2.3 Fuel cell

The fuel cell model implemented in the type 170 is composed of an electrochemical, a thermodynamic and a thermal model. Different outputs are calculated: the stack temperature, the electrical production and the gas consumption.

The electrochemical model is based on different works (Amphlett et al., 1996; Ulleberg 1998). The voltage of a single cell is:

$$U_{\text{cell}} = E + \eta_{\text{act}} + \eta_{\Omega} \quad (\text{eq. 2})$$

where E is the thermodynamic potential given by Nernst equation,  $\eta_{\text{act}}$  is the anode and cathode activation over-voltage and  $\eta_{\Omega}$  the ohmic over-voltage, quantifying the transport losses due to the proton conductivity.

The thermodynamical model has been set up to establish the inlet flowrates for the oxygen  $\dot{n}_{\text{O}_2,\text{in}}$  and hydrogen  $\dot{n}_{\text{H}_2,\text{in}}$ , according to Faraday's law. With this law the real consumption of the gas considering the stoichiometrical coefficients  $S_{\text{H}_2}$  et  $S_{\text{O}_2}$  are calculated:

$$\dot{n}_{\text{H}_2,\text{in}} = S_{\text{H}_2} \frac{N_{\text{cell}} I_{\text{FC}}}{n.F} \quad \text{and} \quad \dot{n}_{\text{O}_2,\text{in}} = S_{\text{O}_2} \frac{1}{2} \dot{n}_{\text{H}_2,\text{cons}} \quad (\text{eq. 3})$$

The stack temperatures  $T_{\text{stack}}$  are evaluated according to the thermal model where  $c_t$  is the thermal capacity of the stacks:

$$c_t \frac{dT_{\text{FC}}}{dt} = Q_{\text{gen}} - Q_{\text{loss}} - Q_{\text{cool}} - Q_{\text{evap}} \quad (\text{eq. 4})$$

$Q_{\text{gen}}$  is the heat generated by the fuel cell,  $Q_{\text{loss}}$  the heat dissipated in the environment,  $Q_{\text{evap}}$  the heat dissipated by evaporation at the cathode and  $Q_{\text{cool}}$  the heat dissipated thanks to an auxiliary.

The principal parameters used for one stack are listed in the table below (Tab. 2) where the eventual connections between parameters and other types are indicated.

Table 2: Elements of the model

Characteristic elements /parameters			Inputs			Outputs			
Number of cells per stack	$N_{\text{cell}}$	100	Control signal	$\delta$	$\delta = (P_{\text{FC}} > 0)$	Power stack	per	$P_{\text{stack}}$	Graph (Type 65)
Number of stacks	$N_{\text{stack}}$	4	Intensity of the cell	$I_{\text{FC}}$	$I_{\text{FC}} = f(V, P_{\text{FC}})$	Current (stack)		$U_{\text{stack}}$	Graph (Type 65)
Electrodes surface	$A_{\text{PEM}}$	400 cm <sup>2</sup>	Input pressure	$p_{\text{gaz,in}}$	1.5 Bars	Gas consumption		$\dot{n}_{\text{H}_2,\text{in}}$	H <sub>2</sub> tank
Ambient temperature	$T_{\text{amb}}$	Inputs (Type 9)	Stoichiometric coefficients	$S_{\text{gaz}}$	1.15 (H2) ; 2.5 (O2)			$\dot{n}_{\text{O}_2,\text{in}}$	O <sub>2</sub> tank
Connexion to TrnSys Types			Input temperature	fluid	$T_{\text{cool}}$	Inputs (Type 9)	Heat	Q	$T_{\text{out}} = f(T_{\text{in}}, Q)$
Constants			Set point temperature in the stack	$T_{\text{stack}}$	Macro Fan				
Connexion to Calculators			Set point temperature in the stack	$T_{\text{stack}}$	70 °C				

### 3.2.4 Turbofan

The turbofan has been modelled associating it to a dissipating cooling system. This system depends on an all or nothing controller. The heat dissipated by the fan is a function of the set point temperature and the flowrate.

The turbofan is composed of a very long heat exchanger of 500 m of 13 mm of diameter with a fin and two fans. There is no existing model in the TrnSys library able to model this kind of turbofan, so that a macro has been developed composed of a pump (Type 3b), managing the water flowrate in the pipe (Type 31) where the sizes are the one of the heat exchanger. The effect of the fins allows increasing the contact area, and therefore increasing the conduction transfer. In the model, the thermal loss coefficient of the pipe is increased so that the conduction transfers due to the fins are well modelled. The cooling of the fluid is accelerated by using fans. This phenomenon is modelled by using a resulting temperature: it corresponds to the outside air temperature adjusted with a negative offset. The resulting temperature is used only when the set point temperature ( $T_{sp} = 35 \text{ }^\circ\text{C}$ ) is overpassed by at least  $2^\circ\text{C}$  ( $\Delta T_+ = 2 \text{ }^\circ\text{C}$ ) and is not used when the temperature is under the set point temperature by  $3 \text{ }^\circ\text{C}$ :  $T = T_{sp} - \Delta T_-$  where  $\Delta T_- = 3 \text{ }^\circ\text{C}$

The parameters  $\Delta T_+$  and  $\Delta T_-$  are the dead-bands of the fans regulator which is at the origin of the oscillations seen on the temperatures measured by the sensors when the fuel cell operates.

## 4. Simulation Results

### 4.1 Electrical outputs

The electrical characteristics of the fuel cell and its sizes are implemented in the Type 170 (Tab. 2). With these parameters we have plot the current–voltage (I–U) characteristics of the PEM fuel cell (Fig 4). This simulation has been compared to the measurements. The measurements stem from a test (blue curve) while the fuel cell was operating in a dynamic mode during 8 hours. We have also represented the I-U curve of this stack, initially characterized (red curve). We can notice that the voltage simulated is always higher than the measured one. Around the nominal operation of the fuel cell, for a current of 333 A, the measured voltage of a stack was initially of 75.1 and of 74.8 V during the test, whereas it is of 79.5 V in the simulations. The curves  $P_{FC} = f(I_{FC})$  around the nominal power of the fuel cell are very close to each other. For  $I = 333 \text{ A}$ , the electrical measured powers are of 100 kW, against 105 kW for the simulated powers.

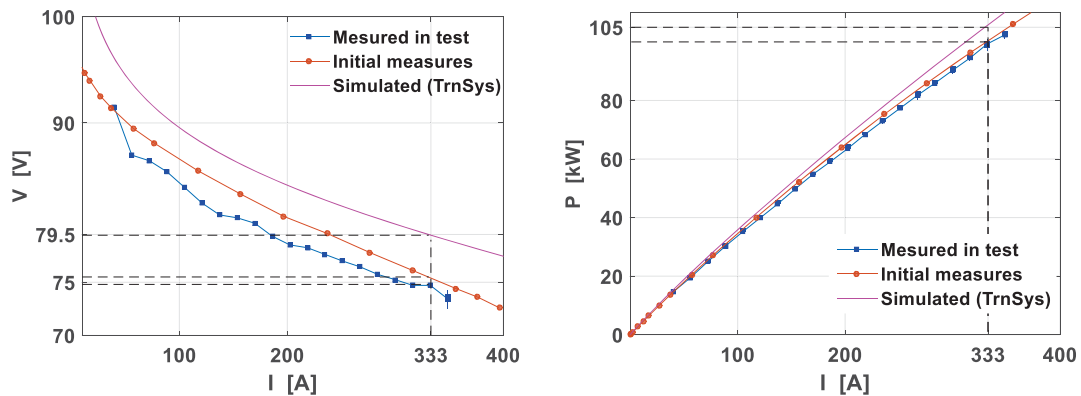


Figure 1: Measured current-voltage curve (blue), current-voltage curve obtained of a stack during the initial characterization (red) and current-voltage curve generated by TrnSys (pink). b.) Current-power characterisation of the fuel cell.

The electrical simulated and measured powers generated by the fuel cell during the period studied are represented on Fig. 5. For both cases, the powers are lower than the powers provided by the curves  $P_{FC} = f(I_{FC})$  of Fig. 4 for  $I = 333 \text{ A}$ . This means that during this period the fuel cell was not used exactly at its nominal capacity. The simulation tends to overestimate the electrical power generated by the fuel cell by 5 to 7 kW: the simulated power is of 100 kW whereas the measured power is of 94 kW. These differences are due to the fact that the measured power is the active power whereas the simulated power is the DC power.

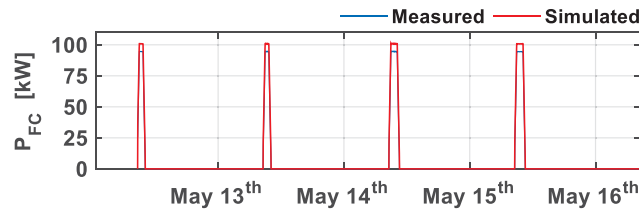


Figure 2: Measured and simulated electrical fuel cell powers

To conclude, the fuel cell type seems correctly parametrized.

#### 4.2 Simulated fluid temperatures

The thermal model and its outputs are the specificity of this model and paper. The outlet water temperatures evaluated by the model after the hydrogen systems, the tank and the turbofan are going to be compared to the measurements with the use of the sensors: KT506, KT507 and KT501 (Fig 6). Whatever the fluid temperature, we focus on if the trends of the simulations are correctly calculated:

1. The simulated temperature increases when one of the hydrogen systems operates. When the fuel cell is on, we can observe oscillations on the KT501 which are due to the turbofan and the valves operation. These oscillations are reproduced by the model but their frequency and phasing are not respected. These results could be improved by characterizing more in detail the control of the turbofan and implementing it in the model. The fluctuations on the simulated temperatures are under evaluated:
  - for KT501: local maximal and minimal temperatures are reproduced with root mean square errors of respectively 1.96 °C and 1.77 °C. These fluctuations are linked to the turbofan regulator bandwidth. These differences show that the limits of the band have to be improved;
  - for KT506, these temperatures are evaluated with root mean square errors of 3.46 °C and 1.77 °C. The heat generated by the model tends to smoothen the inlet temperature;
  - for KT507, the root mean square maximal and minimal errors are respectively of 1.0 °C and 1.71 °C.
2. We see that the temperature decreases due to the thermal losses when no hydrogen system is operating, that is when the water stagnates. These losses are slightly under evaluated by the model. Indeed, concerning the measurements done by KT506, the temperature difference between a moment when the fuel cell starts and a moment when it ends up is of 19.7°C for the first day, of 20.3°C for the second, of 21.5°C for the third and finally of 23°C for the last day. The simulated temperatures show respectively differences of 14.0 °C, 17.2 °C, 11.3 °C and 12.4 °C. When the fuel cell stops operating we can see differences of 8 – 10 °C between simulation and measurement at the KT501 sensor. These differences are mainly explained by the phase shift of the fluctuations produced by the turbofan regulation. At given moments, the measured temperature is at its maximum of the oscillation whereas the simulated temperature is at the minimal.

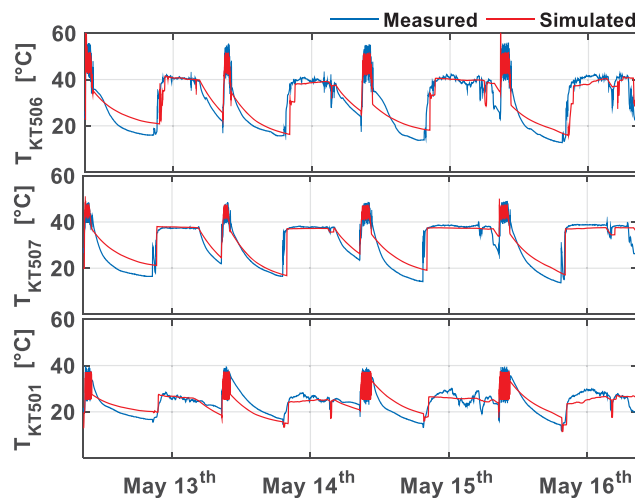


Figure 3: Measured (KT506, KT507 and KT501) and simulated temperatures



#### 4.3 Thermal power

The thermal behaviour of the different elements of the heat recovery system, when the fuel cell operates, is presented on Figs. 7 and 8. Fig. 8 is a boxplot summing up the statistical weights of the heat evaluated: on each box, the horizontal line represents the median, the points is the mean, the vertical line links up the maximum and minimum values, and the horizontal bottom and upper edges of the box are respectively the 25th and 75th percentiles. Thus the spacing between the edges of the box indicates the degree of dispersion of the values.

We can notice that the heat produced by the fuel cell is correctly evaluated: the mean heat produced is of about 70 kW (Fig. 8). However, the fluctuations observed on the measurements are not reproduced by the model when the fuel cell operates at its nominal power. The heat calculated at its nominal power is of about 86 kW whereas the measured power is between 82 and 101 kW.

When the fuel cell reaches its nominal power, the thermal simulated exchanges in the tank are of 15.2 kW against 14.5 kW with the measures (Fig. 8). We notice that the simulated power fluctuates less compared to the measured (between 0-20 kW for the simulation against 0-46 kW for the measurements). This is due to the simulated temperature located after the fuel cell, which is less varying. The simulated heat generated by the fuel cell seems too smooth and stable.

Finally, the thermal dissipated power by the turbofan is slightly under evaluated but acceptable. In average the turbofan model dissipates 54.2 kW whereas the measurements show 55.6 kW. Here, the fluctuations are suitably evaluated.

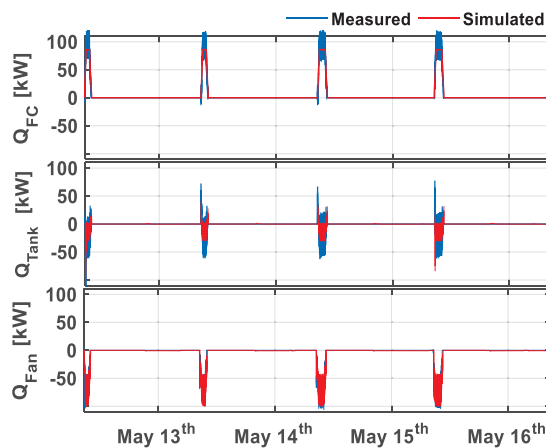


Figure 4: Temporal simulated and measured thermal powers when the fuel cell operates

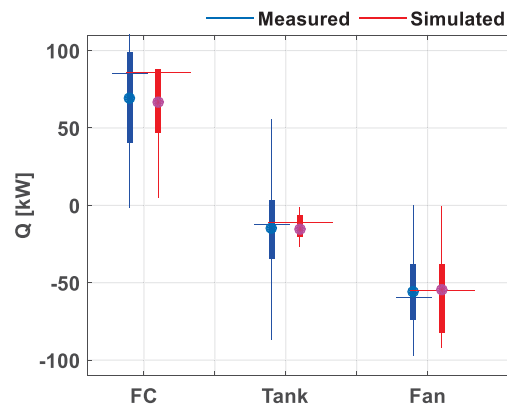


Figure 5: Thermal measured and simulated boxplot powers when the fuel cell operates

To conclude, the model tends to agree with the measurements for both transient temperature and thermal exchanges simulations. Certain aspects need to be improved: the thermal losses on the pipes as well as the tank thermal exchanges. When looking at the transient evolution of the temperatures and heat exchanges we have often noticed that the fluctuations are less well represented with the model.

### 5. Conclusion

The experimental MYRTE platform is dedicated to PV/ hydrogen studies. It is composed of a 560 kW<sub>p</sub> PV array, of a fuel cell with a nominal power of 100 kW, an electrolyzer with a nominal power of 50 kW and a hydrogen flowrate reaching 10 Nm<sup>3</sup>/h. It is composed of hydrogen and oxygen tanks for the storage. The heat generated by the electrolyzer and fuel cell is recovered via the heat recovery system in order to maintain a set point temperature.

This paper focusses on the transient modelling of the heat recovery system. The different sub-models are introduced and the global electrical and thermal performances are presented. First the PEM fuel cell is modelled using type 170 of TrnSys. The model seems to be correctly parameterized: the electrical and thermal outputs agree and are correlated to the measurements. The turbofan seems to reproduce the heat dissipated though its regulation needs to be improved. The losses in the pipes are under estimated by the model but the

global trend is acceptable. Finally, the TrnSys type 60d used for the tank is acceptable but we know that our tank has a particular geometry so further measurements need to be done to characterize the tank model and to know whether we can improve type 60d. The heat generated by the electrolyzer has been measured and the average measured heat generated has been used in the model as an input.

The next step is to model the thermal exchanges in the electrolyzer and to transform it in a TrnSys Type. This model will be based on (Agbli et al., 2011, Gorgun, 2006) works and further measurements will be required to set the current-voltage curves for different operating temperatures. If a more detailed performance of the global model is expected then we will need to work on the regulation of some sub-models in order to increase the transient responses accuracy.

The final aim of this work is to be able to exploit the heat generated by the platform in order to recover it for residential applications. A future study, coupling an efficient building's behaviour and this experimental platform will be done in order to quantify the global energy saving which could be achieved. Also, for the moment, this platform is used for electrical demands, whereas we have seen that the heat generated can be as important as the electricity produced. A future application will be to prioritize the heat and consider electricity as a residual power. Finally, a technical and economic analysis will lead to be able to propose the best application to increase the global platform's energy and exergy efficiency.

## **6. References**

Agbli, K.S., Péra, M.C., Hissel, D., Rallières, O., Turpin, C., Doumbia, I., 2011. Multiphysics simulation of a PEM electrolyser: Energetic Macroscopic Representation approach. *International Journal of Hydrogen Energy* 36, 1382–1398. doi:10.1016/j.ijhydene.2010.10.069

Amphlett J. C., Mann R. F., Peppley B. A., Roberge P. R., Rodrigues A. and Salvador J. P. (1996) A model predicting transient responses of proton exchange membrane fuel cells. *J. Power Sources* 61(1-2): 183-188

Darras, C., 2010. Modélisation de systèmes hybrides photovoltaïque/hydrogène: applications site isolé, micro-réseau et connexion au réseau électrique dans le cadre du projet PEPITE (ANR PAN-H). (PhD, « French »). Università di Corsica Pascal Paoli.

Darras, C., Muselli, M., Poggi, P., Voyant, C., Hoguet, J.-C., Montignac, F., 2012. PV output power fluctuations smoothing: The MYRTE platform experience. *Int. J. Hydrog. Energy* 37, 14015–14025. doi:10.1016/j.ijhydene.2012.07.083

Gorgun, H., 2006. Dynamic modelling of a proton exchange membrane (PEM) electrolyzer. *International Journal of Hydrogen Energy* 31, 29–38. doi:10.1016/j.ijhydene.2005.04.001

Hwang, J.-J., 2013. Transient efficiency measurement of a combined heat and power fuel cell generator. *Journal of Power Sources* 223, 325–335. doi:10.1016/j.jpowsour.2012.09.086

TRNSYS Mathematical Reference, 1996. Solar Energy Laboratory Madison, United States, University Wisconsin.

Ulleberg Øystein, 1998. Stand-alone power systems for the future: optimal design, operation & control of solar-hydrogen energy systems. Norwegian University of Science and technology, Norway.